Shahrood University of Technology

Journal of Mining and Environment (JME)

Journal homepage: www.jme.shahroodut.ac.ir

Iranian Society of Mining Engineering (IRSME)

Simulation of Pyrrhotite Removal from Scheelite Ore by Magnetic Force in Table Concentration

Chol Ung Ryom[1], Kwang Hyok Pak[1], Il Chol Sin[1], Kwang Chol So[1], and Un Chol Han[2]*

1. Faculty of Mining Engineering, Kim Chaek University of Technology, Pyongyang, Democratic People's Republic of Korea
2. School of Science and Engineering, Kim Chaek University of Technology, Pyongyang, Democratic People's Republic of Korea

Article Info

Received 21 July 2023
Received in Revised form 26 August 2023
Accepted 19 September 2023
Published online 19 September 2023

DOI: 10.22044/jme.2023.13397.2469

Keywords

Table concentration
Scheelite
Pyrrhotite
Magnetic bar
CFD simulation

Abstract

Scheelite ore with heavy and magnetic minerals can be generally concentrated using shaking table centered gravity-magnetic processing. When magnetic field is formed by fixing magnetic bars on which permanent magnets are arranged at a constant interval, above the table desk, heavy scheelite particles can be concentrated by gravity, whereas heavy magnetic mineral particles can be floated off like light mineral particles by upward magnetic force. In this paper, concentration of scheelite and removal of pyrrhotite floated by magnetic force was simulated using CFD for the sample containing 1% scheelite and 2% pyrrhotite, and compared with the experiment. As a result, WO3 grade and separation efficiency of concentrate were 65.3% and 80.1%, respectively, in the new table equipped with magnetic bars, whereas 28.4% and 76.5%, respectively, in conventional table. The magnetic field formed by fixing magnetic bars above table could be significant in simplifying the sequential tabling-magnetic separation process and reducing the loss of scheelite.

1. Introduction

Gravity, flotation, and magnetic concentration are the main beneficiation techniques, which are most commonly applied to concentration of scheelite [1]. Scheelite ores which are often found in tungsten deposits such as skarn occasionally include other valuable sulfide minerals [2, 3].

Scheelite is mineral of tungsten. Tungsten, also known as wolfram, with symbol W, has the highest melting point of all metals (3422 ± 15 °C). With its density of 19250 kg/m3, tungsten is also among the heaviest metals. Tungsten has a wide range of applications in industry such as high-temperature technology, the chemical industry, lighting, X-ray technology, and superalloys. Tungsten features the lowest vapour pressure of all metals, very high moduli of compression and elasticity, very high thermal creep resistance, and high thermal and electrical conductivity.

Tungsten is the most important metal for thermo-emission applications, not only because of its high electron emissivity, which is caused by trace additions of other elements, but also because of its high thermal and chemical stability. Tungsten usually contains small concentrations of carbon and oxygen, which impart considerable hardness and brittleness.

Cemented carbides, also called hard metals, are the most important applications of tungsten today. Tungsten monocarbide (WC) is the main constituent and has a hardness close to diamond. Hard metal tools are used for the shaping of metals, alloys, ceramics, and other materials.

About 54–72% of the tungsten produced globally is used for hard metals. Steel and alloys, mill products such as lighting filaments, electrodes, electrical, and electronic contacts, wires, sheets, rods, and a widespread variety of chemicals represent other important uses of tungsten.

* Corresponding author: huch8272@star-co.net.kp (U.C. Han)

Tungsten has also high wear resistance and good X-ray performance. Beside, some tungsten compounds of are used in production of fluorescent material, paint, dye, tanning agent, fire prevention cloth, etc. [1, 3, 4].

The most innovative studies in the recent years on scheelite beneficiation have mainly focused on selective flotation separation of scheelite from other minerals containing calcium such as calcite by using reagents of better selectivity, and optimization of concentration of complex scheelite ores through combining gravity, magnetic and flotation separations, and recovering associated valuable sulphides [1, 4].

The optimization of designing gravity concentration circuits for scheelite had been described in detail, jigs, spirals, shaking tables, and centrifugal concentrators are often used in scheelite concentration, and especially, shaking tables are needed for final separation.

Fine grounded scheelite ore is generally separated in shaking table [5, 6]. Later table concentration, flotation or magnetic concentrations are generaly used to scheelite concentration.

Flotation is needed not only to separate the fine scheelite particles that cannot be recovered by gravity concentration [7, 8], but also to recovery useful metals and remove impurities in scheelite ores [9].

Magnetic separation is applied for removing and recovery of magnetic minerals with high density in scheelite ore. The similarity between scheelite and pyrrhotite in their densities makes the gravity separation more difficult and decreases the grade of scheelite concentrate.

Pyrrhotite (Fe(1-x)S) is one of most general metal sulphide, which is non-stoichiometric compounds, where x value is $0 \leq x \leq 0.125$ [10]. Pyrrhotite is iron sulphide mineral with ferrimagnetism, and is chemically unstable in high temperature. The Curie temperature of pyrrhotite is 320 0C, where it decomposes to magnetite [11]. Most of pyrrhotites are Fe7S8, which have monoclinic structure and ferromagnetic in nature. Some of pyrrhotites have hexagonal structure, but our study focused on ferromagnetic pyrrhotite. Pyrrhotite is generally more strongly magnetic than hematite, and the saturation polarization, at room temperature, is becoming to magnetic product in 0.12 T of magnetic field [12].

Generally, if there are great amount of pyrrhotites in scheelite ore, pyrrhotites are removed by magnetic separation, and then scheelites are separated by gravity separation, and are, respectively, sent to the consumers. If there are small amount of pyrrhotites in scheelite ore, pyrrhotite is separated by gravity-magnetic separation processing and throwed away.

Scheelites are blended in magnetic flocculation in magnetic processing, therefore, scheelites will be lost.

Shaking table is a gravity concentrator to separate minerals in the thin water film that flows over a inclined plane using difference of minerals in their densities and it is used to separate tungsten, tin, iron, tantalum, barium, titanium, zirconium, and to a lesser extent, gold, silver, thorium, uranium [13], and now also used in recycling of packaging plastics [14].

The separation on a shaking table is controlled by a number of operating variables such as wash water, feed pulp density, deck slope, strokes per minute, length of stroke, and feed rate, and the importance of these variables in the model development is discussed [15 ~ 18].

The significance of the many design and operating variables and their interactions have been reviewed by Sivamohan and Forssberg [15], and the development of a mathematical model of a shaking table has been described by Manser [16].

Fine scheelite particles are heavy, so they flow into concentrate launder, and light minerals such as quartz and calcite are washed into tailing launder by water flow in table. As the iron sulfides such as pyrrhotite are heavy, they may flow into the concentrate launder, therefore, degrading of scheelite concentrate.

Figure 1 shows the magnetic bar fixed in shaking table.

Straight magnetic bar on which permanent magnets were arranged at a constant interval, were fixed at a certain level on the table desk.

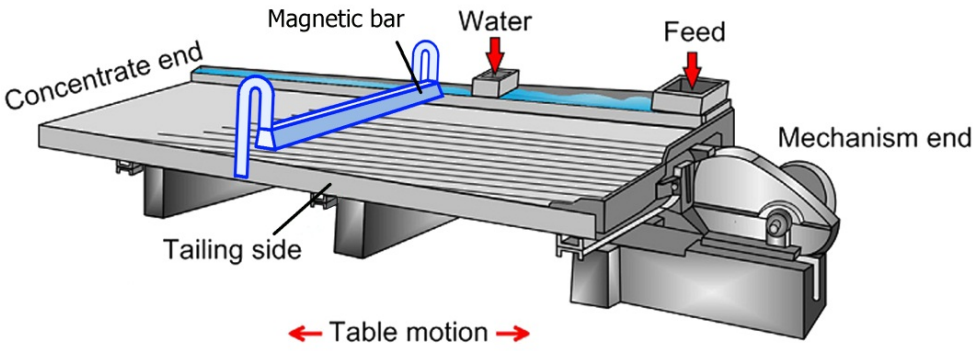

Figure 1. Magnetic bar fixed on table desk.

Permanent magnets were arranged on the magnet fixing frame above the desk rather than on the desk back, forming magnetic field (Figure 2). Magnetic bars were fixed in the direction horizontal but normal to the riffles.

The magnetic force of magnetic bar pulled upward magnetic particles on table desk. Magnetic mineral particles were floated in water or on water surface by magnetic force of magnetic bar, and washed off into tailing with light minerals by water flow (Figure 2).

There could be magnetic flocculation during separation, but it had a small size because the magnetic force exerting on mineral particles was rather weak. Besides, shaking motion of table desk also prevented scheelite particles from enclosing with magnetic flocculation chain, thus reducing loss ratio of scheelite.

To remove pyrrhotite successfully, pyrrhotite particles should be not attactted to magnetic bar surface, but floated to the water surface and washed with light minerals by water flow. Magnets arrange distance and postion of magnetic bar should be set resonably to achive this.

The forces acting on mineral particle are magnetic force F_{mag} (magnetic force act into magnetic minerals) and drag force $\sum F_{drag}$ (Figure 2).

Drag force $\sum F_{drag}$ is sum of other forces, which $\vec{F}_g$ is gravity force; $\vec{F}_{buo}$ is buoyant force, etc., and can be written as last a term in formula 6.

Magnetic force F_{mag} acted on pyrrhotite can be described as following [13, 19]:

$$F_{mag} = \frac{1}{2}\mu_0 V_p \chi \nabla H^2 \quad (1)$$

where F_{mag} is magnetic force acted pyrrhotite, μ_0 is magnetic constant, V_p is the volume of particle, χ is the magnetic susceptibility of pyrrhotite, H is intensity of magnetic field, and ∇H is gradient of intensity of magnetic field.

Intensity of magnetic field and magnetic gradient in open-circuit magnet system depend on arrangement of permanent magnets [13, 19].

Conditions to float magnetic mineral particles and not to attach to magnetic bar are following as:

Firstly, magnetic force $F_{f.mag}$ acting to magnetic particles is larger than drag force $\sum F_{drag}$, which is sum of $\vec{F}_g$, $\vec{F}_{buo}$, etc. in bottom of desk, therefore, pyrrhotite can be floated (formula 2).

$$F_{f,\ mag} > \sum F_{drag} \quad (2)$$

where $F_{f.mag}$ is magnetic force acting to magnetic particles.

Secondly, when magnetic force acting on magnetic particles is smaller than sum of $\sum F_{drag}$ and surface tension of water-air F_{sf} in water or water surface, so that pyrrhotite can be not attact to magnetic bar and washed with water (formula 3).

$$F_{sf} + \sum F_{drag} > F_{f,\ mag} \quad (3)$$

where F_{sf} is surface tension of water-air surface.

In such conditions, heavy pyrrhotite particles can be floatted and render to tailing, therefore, grade of scheelite concentrate will be raised.

Fixing magnetic bar over desk, i.e. combination of gravity separation and magnetic separation allows scheelite concentration and pyrrhotite removal to be simultaneously accomplished, so following magnetic separation for pyrrhotite removal is not necessary. It is the aim of this study.

Hence, the possibilitys of concentration of scheelite and removal of pyrrhotite into tailing without attatching to the magnetic bars, should be proved through simulation and experiment.

This study belongs in combine the force of gravity with a magnetic force in gravity separater. Although the initial efforts to combine gravity with magnetic separation began in the middle of the last century 80`s, their success has been limited [19]. Permanent magnets placed under the separating surface in spiral and shaking table can be arranged so that an intermittent or a moving magnetic field permits removal of the magnetic material to the concentrate discharge slot [20]. In spite of obvious advantages and often promising results, the technique has not found a wide-spread application in mineral processing.

The basic idea of combining gravitational and magnetic fields in the jigging process for separation of fine particles was proposed and the physical principles of process outlined by Lin [20~22].

Shaking table with magnetic bar had been used before in the retreatment of concentrate of alluvial gold dressing.

In the recent years, CFD (Computational Fluid Dynamics) has been widely used in simulation of phenomena which take place in fluid media of gravity concentrtion.

In the field of gravity concentrator, CFD had been used for simulation of particle flows in hydrocyclone [24, 25], jigs [26, 27] and thickener [28]. Research has simulated the process of separation in Knelson concentrator using CFD [29]. In this syudy, **realizable mixture** k-ε turbulence model has been selected to model the turbulence of fluid phase due to its swirling nature.

Using CFD-DEM, segregation [30] of a multi-dispersed population of grains in vibrating table was simulated and combined qualitative and quantitative assessments of process conditions such as deck shape, and new formal vibrating table gravity concentration [31, 32] was researched.

However, there is no enough information on the CFD simulation of gravity concentration, especially in water medium on the shaing table.

In this study, the separation of scheelite, pyrrhotite, and quartz particles on the conventional table and table with magnetic bars were simulated with CFD. The simulation results were compared with the experiment results.

2. Modeling for CDF Simulation

2.1. Model of CDF simulation

In order to study the flow behavior of the different phases, continuity equation and momentum balance equations for each phase was formulated. Both the solid phases have been treated as continua. The unsteady state continuity equation for the fluid/solid phase ***i***, can thus be written as literature [33]:

$$\frac{\partial \alpha_i}{\partial \mathrm{t}} + \nabla \cdot (\alpha_i V_i) = 0 \quad (4)$$

where α_i is the volume fraction of i_{th} phase (solid or liquid), and V_i is the velocity vector of the i_{th} phase.

The momentum equation for the liquid phase ***l*** is given as:

$$\frac{\partial(\rho_i \alpha_{ki} V_i)}{\partial t} + \nabla \cdot (\alpha_l \rho_l V_l V_s) = -\alpha_k \nabla p + \nabla \cdot \bar{\bar{\tau}}_l + \alpha_l \rho_l g + \sum_{s=1}^{2} k_{sl} (V_s - V_l) \quad (5)$$

where $\boldsymbol{g}$ is the acceleration due to gravity, $\bar{\bar{\tau}}_l$ is the stress tensor for the l_{th} phase, and $\nabla \mathrm{p}$ the pressure gradient, K_{sl} the interaction coefficient between the liquid and the solid phase.

The solid momentum balance equation for the particles can be written:

$$\frac{\partial(\rho_s \alpha_s V_s)}{\partial t} + \nabla \cdot (\alpha_l \rho_l V_l V_s) = -\alpha_s \nabla p - \nabla p_s + \nabla \cdot \bar{\bar{\tau}}_s + \alpha_k \rho_k g + F_{mag} - \sum F_{drag} \quad (6)$$

where $\bar{\bar{\tau}}_s$ is the stress tensor for the solid phase, p_s is the pressure due to the solids, F_{mag} is magnetic force, $\sum \mathrm{F}_{\mathrm{drag}}$ is sum of other forces, which $\vec{\mathrm{F}}_{\mathrm{buo}}$ is buoyant force, $\vec{\mathrm{F}}_{\mathrm{wl,q}}$ is wall inner friction, $\vec{\mathrm{F}}_{\mathrm{vm,q}}$ is virtual mass force, $\vec{\mathrm{F}}_{\mathrm{td,q}}$ is

turbulent force, $\vec{R}_{pq}$ is interaction fore between phases,$\vec{v}_{pq}$ is interaction velocity of phases.

In order to predict the multiphase flow, the **Eulerian** model is used, and the standard $k-\varepsilon$ model is selected to model the turbulence of fluid phases. The governing Navier-Stokes equations were solved under **the pressure-based**, **unsteady state**, and **double precision** conditions.

2.2. Boundary condition of simulation

The discretization of governing equations is done by finite volume solver available in the CFD. The geometry of the shaking table was created and the meshing of the domain was done using the commercial software.

Simulations were done with Wilfley table which is widely used in mineral processing. The plant size table had a length of 4500 mm, and a width of 1800 mm. Although the laboratory size table had a length of 1000 mm and a width of 400 mm, it could reflect the result from former table enough. Hence, all simulations and experiments were done with the laboratory size.

In Figure 3, inlet was set as feed area and wash water area, outlet was set as concentrate area and tailing area.

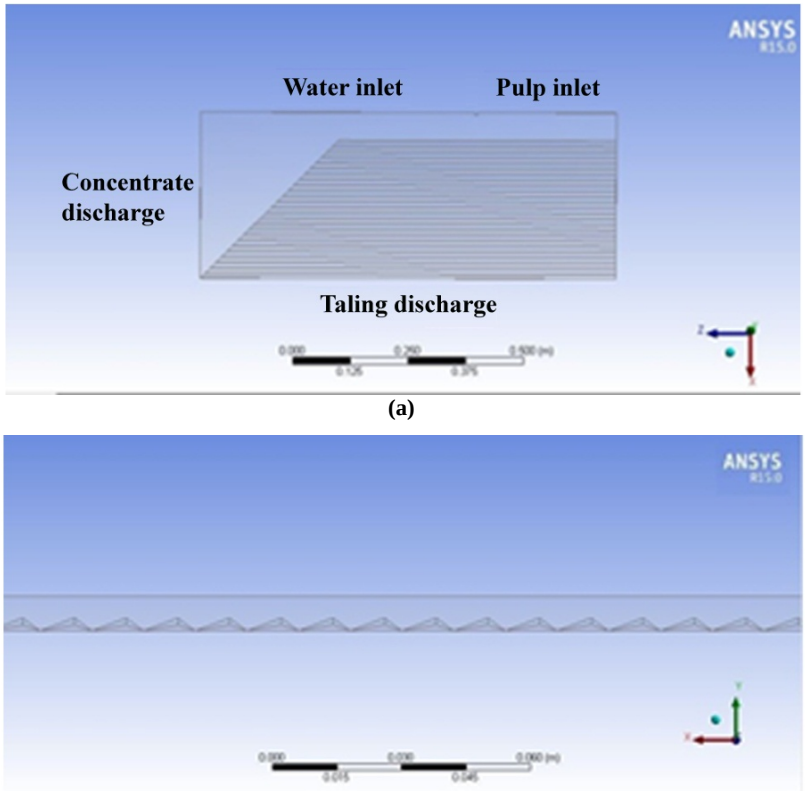

Figure 3. Geometric model of shaking table. a) Table desk; b) riffels.

The length of the table was 900 mm, width was 360 mm, interval of riffles was 12 mm, height of riffles was 3 mm, and longitudinal direction slop angle was 0 degree in simulation. Height of riffles is low and taper away from mechanism to concentration area.

The geometry of table desk was so relatively complex that tetrahedral and mixed cell was created on the entire domain using **ANSYS ICEM CFD**. The 3D model and domain was meshed with a structured mesh consisting of 361870 nodes. Model of meshed node is in Figure 4.

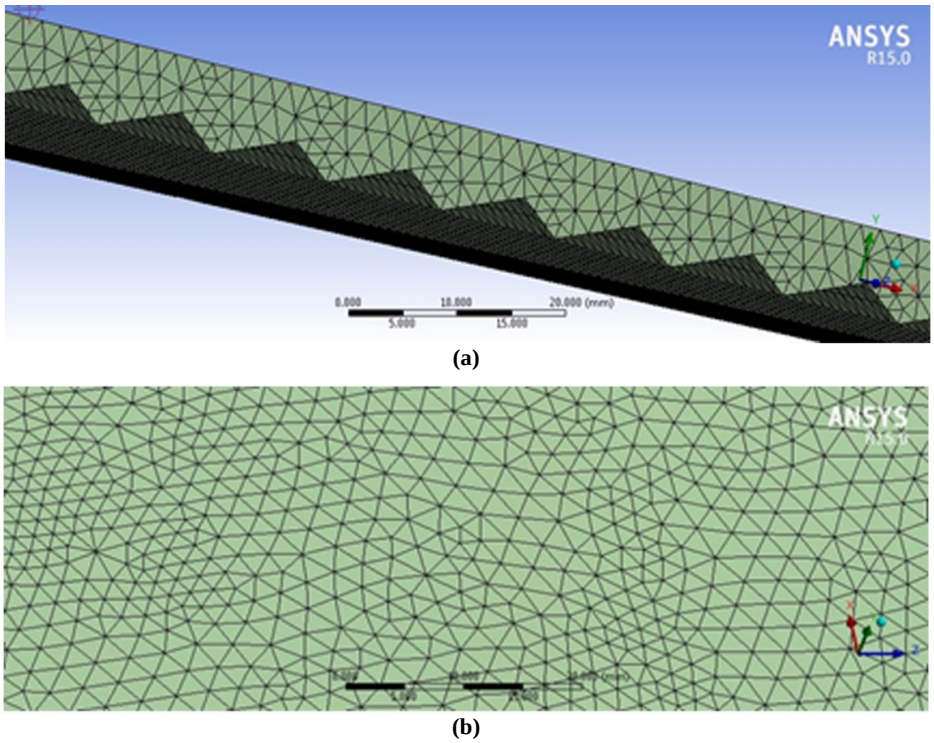

(a)

(b)

Figure 4. Model of mesh. a) Mesh in riffles; b) automatic mesh.

When we considered accuracy of solution and computation, the value of minimum **orthogonal quality**, **maximum skewness**, **and maximum aspect ratio** were 0.532, 0.1665, and 5.236, respectively, these values were estimated the relatively high quality of mesh.

Four phases are considered as one liquid phase and three solid phases. Solid feed material is considered mixture of scheelite, pyrrhotite, and quartz. The water is 1th phase, other is 2th phase, and density of water is 1000 kg /m^3, scheelite 6000 kg /m^3, pyrrhotite 4600 kg /m^3, quartz 2650 kg /m^3.

First, a steady state solution is obtained using the **mixture** model, and then unsteady state simulation is performed using the **Eulerian** model under the existence of magnetic field. **Phase-coupled SIMPLE** algorithm is used for **pressure-velocity coupling**.

First order upwind scheme is used for the discretization of the physical quantities including momentum, turbulent kinetic energy, turbulent dissipation rate, and least squares cell-based is used for the spatial discretization method of gradient. The under relaxation factors are set as 0.7 for pressure, 0.1 for momentum and 0.6 for volume fraction.

Simulation of table separation process for the multiphase flow is carried out for 10 s. Time step is very important to get a convergence. If time step is too large, it is difficult to converge and if it is too small, computational time increases. In this simulation, by considering accuracy and computational cost, the value of time step is selected to 0.005 s.

The boundary conditions at the inlet are set to velocity-inlet, velocity of feed pulp and wash water is set as 0.1 m/s, respectively, and the direction of flow is normal to inlet surface. In simulation, there was content of scheelite 1%, content of pyrrhotite 2%, content of quartz 2%. The boundary conditions at the outlet are set to pressure-outlet, gradient of all variables are taken to be zero and the pressure is considered to be atmosphere. At the walls, **moving wall** conditions are assumed to predict the reciprocating motion of the shaking table desk by interrupting UDF.

Boundary parameters used in this simulation are given in Table 1.

Table 1. Boundary conditions

Index	Specification	Units	Value
Input	Velocity inlet (pulp)	m/s	0.1
	Velocity inlet (wash water)	m/s	0.1
Output	Pressure output	MPa	0.1
Wall	Strokes per minute	rpm	300
	Length of stroke	mm	12
	Velocity of desk	m/s	UDF
Content of ore	Scheelite	%	1
	Pyrrotite	%	2
	Quartz	%	97
Size	Ore (feed size)	mm	0.5 ~ 0.04
Flow media	-	-	water, multi-fluid

Table desk slowly move forward, while it quickly move back. As a result, forward movement accelelation and backward accelelation of table desk are different each other, and materials on the desk by inertia advance forward direction to concentrate side.

The model of motion velocity of desk is as following:

$$v_{ta} = 0.5L\omega(\sin \omega t - 0.5\lambda \sin 2\omega t) \quad (7)$$

where v_{ta} is the velocity of table desk, ω is the shaking angular velocity and equals $\omega = \pi n/30$, n and L are the shaking number and distance of desk, repectively, and λ is the ratio of forward acceleration and backward acceleration of desk, and equals to 2. Velocity of table desk is given by using UDF function. Because volume ratio of each phasis was changed according to time during separation, it was non-steady flow model.

3. Results of Simulation

3.1. Simulation results of gravity concentration

The model equations were solved for the entire domain with the boundary conditions given using the commercial CFD software.

First, simulation for concentration of the mineral particles on the shaking table without any magnetic feild was carried out. At outlet, the velocity and the concentration gradient for all the phases are taken to be zero and the pressure is considered to be atmospheric. At the inlet, the velocity and volume fraction of all the phases are specified.

In order to get a converged solution the **under-relaxation factors** were kept at **0.3 for pressure**, 0.7 **for momentum**, **0.8 for turbulent kinetic energy**, 0.8 **for turbulent dissipation rate**, and the others were 1.

Size of feed is generally – 250 μm in concentration table [5], parameters such as deck slope, strokes per minute, length of stroke, feed rate, and rate of wash water were already determined in scheelite concentration [15, 16]. Simulation was carried out in condition of quantity of water 4.8m^3/h, deck slope 2°, strokes per minute 300 mm, length of stroke 12 mm, and feed rate 1.0 t/h.

Figure 5 are simulation results of scheelite concentration, while Figures 6 and 7 are the simulation results of pyrrhotite and quartz particles, respectively.

As shown in Figure 5, scheelite was placed on the top area of table at the beginning of simulation, and as time went by, it started to be concentrated into the space between riffles reaching upper middle area of the table at 6 s. It reached the riffle-less area for concentrate at 10 s. The simulation of scheelite separation is exactly described in the concentration process in the table.

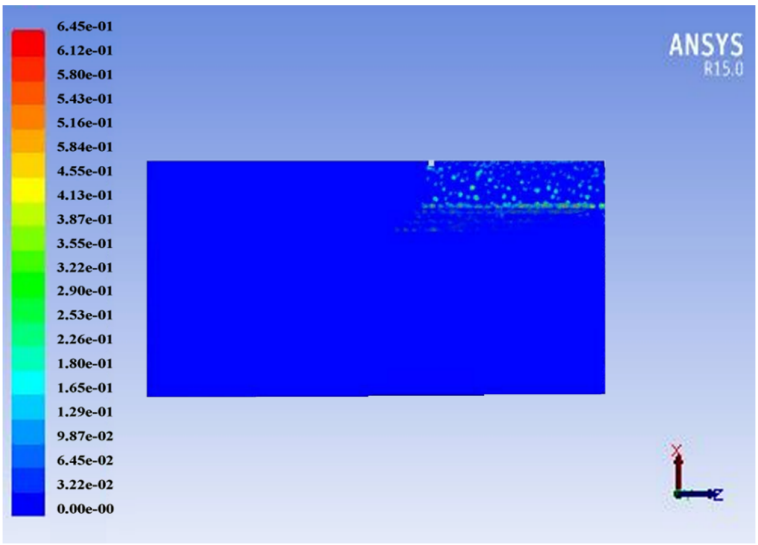

(a)

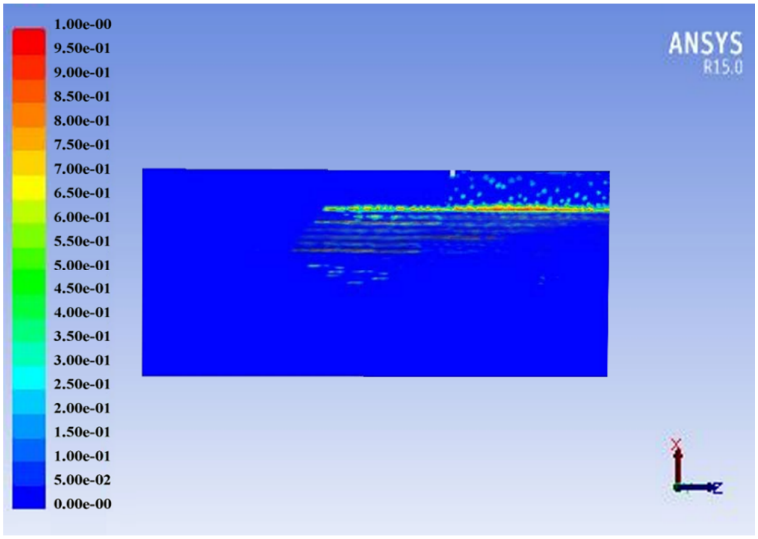

(b)

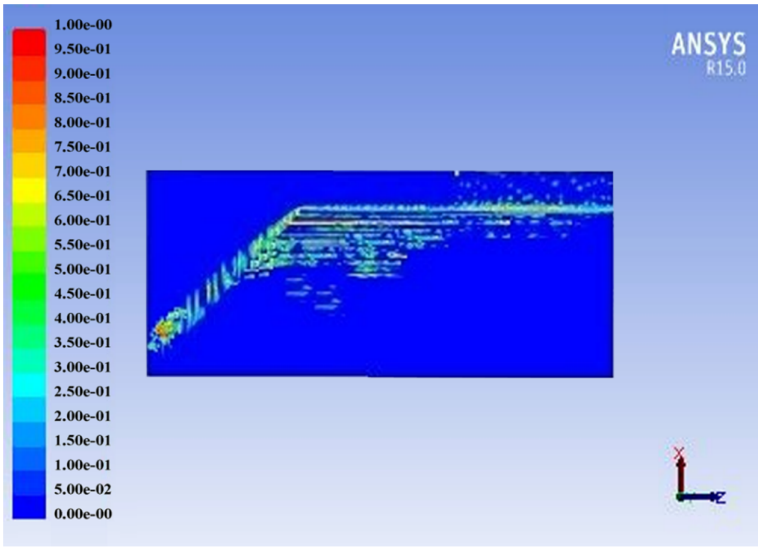

(c)

Figure 5. Result of simulation of scheelite. 4) Time, 1 s; b) time, 6 s; c) time, 10 s.

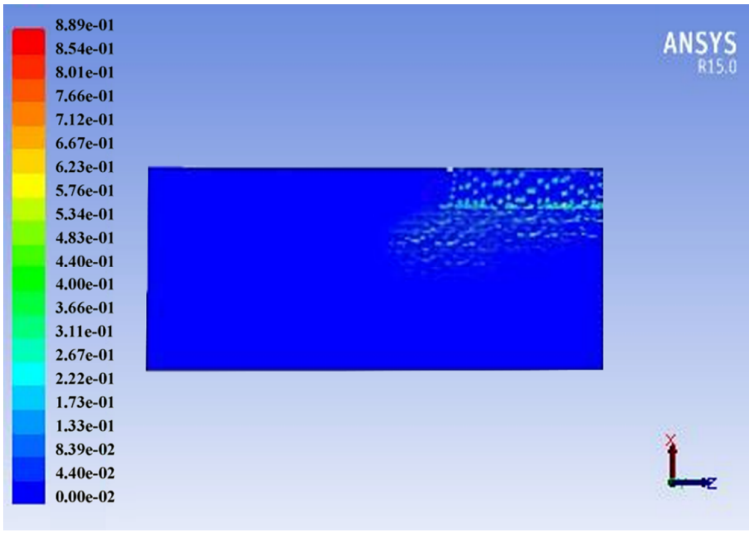

(a)

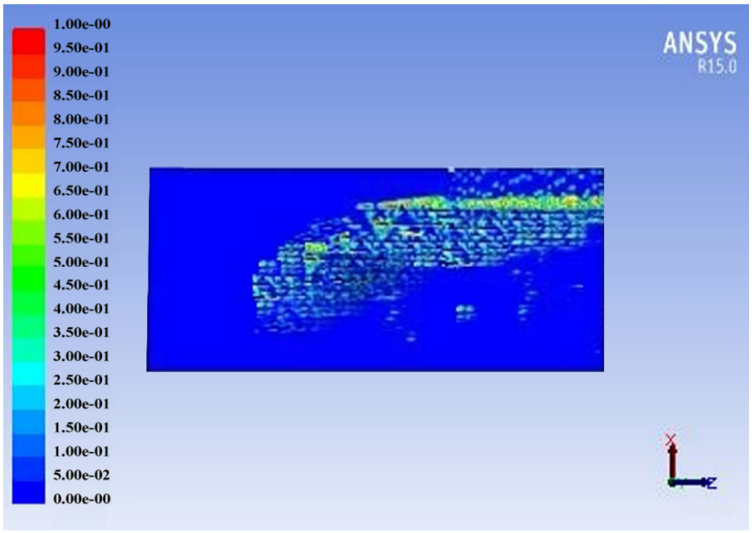

(b)

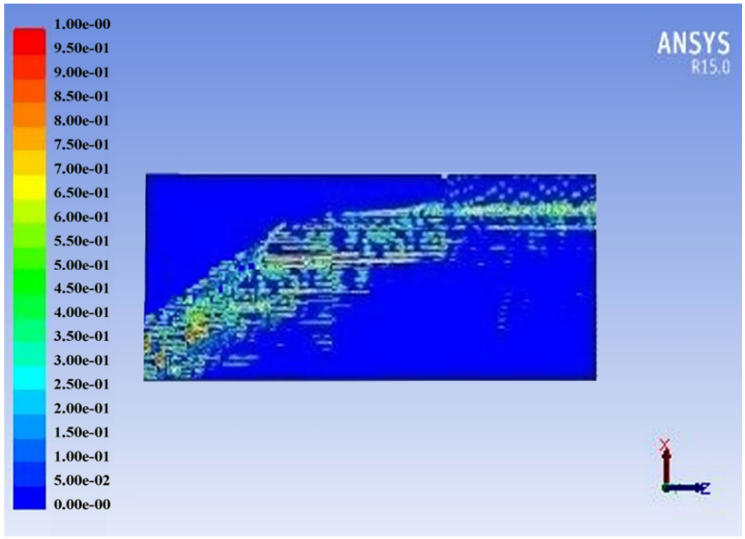

(c)

Figure 6. Result of simulation of pyrrhotite. a) Time, 1s; b) time, 6 s; c) time, 10 s.

Pyrrhotite was twice as much as scheelite. As shown in Figure 6, because pyrrhotite also belongs to heavy mineral, it was concentrated between riffles to enter the concentrate area at 10 s. The simulation of pyrrhotite separation also showed exactly the gravit concentration process of heavy mineral.

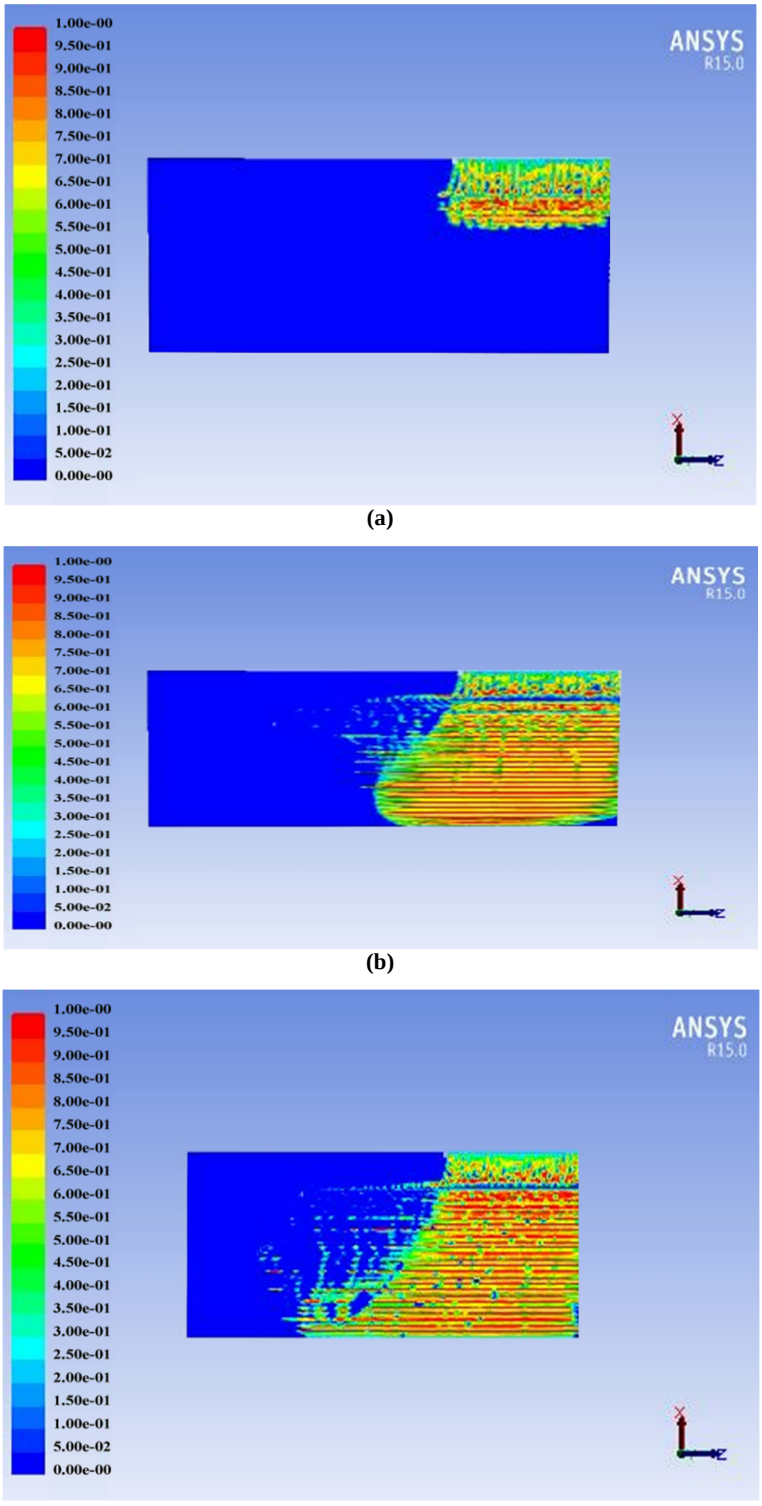

(a)

(b)

(c)

Figure 7. Result of simulation of quartz. a) Time, 1s; b) time, 6 s; c) time, 10 s.

Quartz took the largest part of the feed. As shown in Figure7, because it belongs to light mineral, it was placed in the feeding area of table at 1s and in the central area at 6s. Finally it was washed into the tailing area at 10s. Even though simulation time increased, most of quartz went to the tailing area except for small amount of it that reached the concentrate area.

On the whole, scheelite and pyrrhotite, which are heavy mineral flow to concentrate, but light mineral –quartz flows to tailing. 97% of scheelite, 95% of pyrrhotite, and 3% of quartz in feed is collected to concentrate.

Contours of volume fraction for scheelite and quartz particles in riffle space are shown as Figures 8 and 9, respectively.

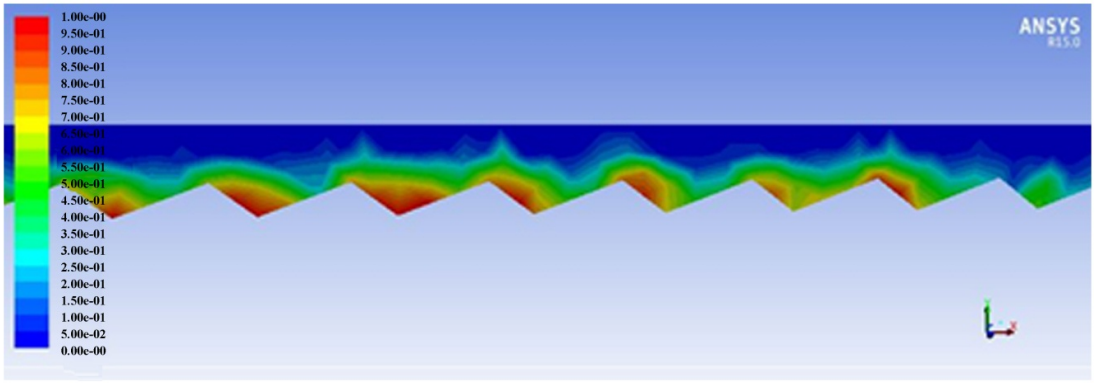

Figure 8. Contours of volume fraction of scheelite particles in riffles.

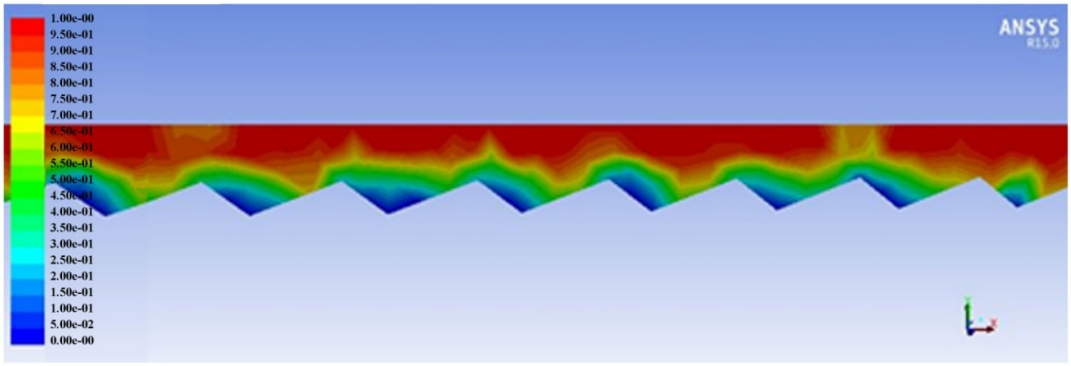

Figure 9. Contours of volume fraction of quartz particles in riffles.

As shown in the above figures, scheelite particles were concentrated in spaces between riffles, light mineral particles such as quartz were washed to tailing over riffles. It should be noted that concentration of heavy minerals was clearly processed.

3.2. Simulation of pyrrhotite removal by magnetic force

Secondly, motion simulation of the pyrrhotite particles when magnetic field on table desk was carried out.

Magnetic character of pyrrhotite also was considered in simulation. Specific magnetic susceptibility of pyrrhotite increases according to increasing of outside magnetic field and particle sizs, its value is $4 \times 10^{-5} \sim 7 \times 10^{-5}$ m^3/kg, maximum of specific magnetic susceptibility is 7×10^{-5} m^3/kg in 0.03 **T** magnetic induce [34].

Specific magnetic susceptibility of pyrrhotite increases as outside magnetic field and particle size increase, its value is $4 \times 10^{-5} \sim 7 \times 10^{-5}$ m^3/kg, maximum of specific magnetic susceptibility is 7×10^{-5} m^3/kg in 0.03 T magnetic induce [34].

Property of magnet was also considered in simulation. Magnet bar can be made with ferrite, samarium-cobalt magnet Sm-Co, neodymium-iron-boron magnet Nd-Fe-B can be arranged in. If ferrites with weak magnetic field are arranged, fixing height is very low, but if rare earth magnets with high magnetic field are arranged, setting height is very large.

Use of Samarium-cobalt magnets has economical advantage, therefore, these magnets

were used. Magnetic property of magnet Sm_2O_{17} is residual magnetization B_r - 1.1 T, coercive force H_c - 10.0 KOe, H_{ci} -33.0 KOe, maximum energy product $(BH)_{max}$ - 300.0 KJ/m^3 [35].

As shown, permanent magnets were arranged with certain distance at certain height over the desk of table. Permanent magnets with length 50 mm, width 25 mm, thickness 10 mm arranged on mounting bar and it is set in position of feed side end on table desk.

Geometric model of permanent magnets arranged is shown in Figure 10.

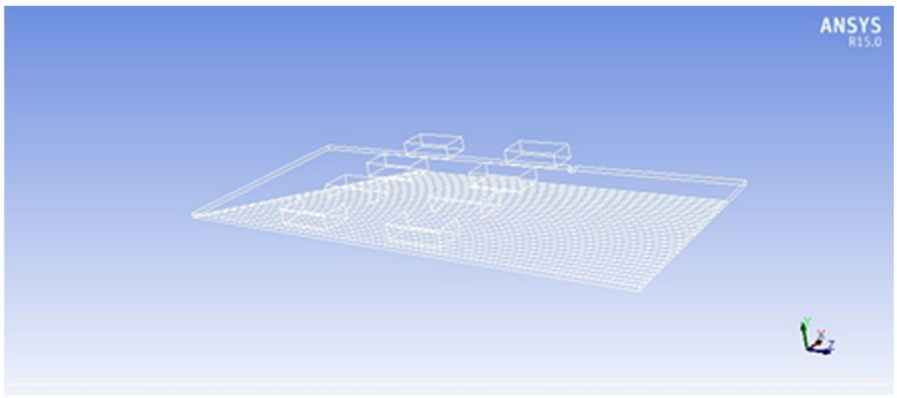

Figure 10. Geometric model of permanent magnets arranged.

Major factors in simulation are the size of pyrrhotite fed on table, setting height of magnetic bar, and arrangement space of magnets on magnetic bar.

Firstly, size of pyrrhotite was considered in simulation. The grinding size is determined according to scheelite grain size, which affects on concentration. Inpractice, size of pyrrhotite particle processed is similar to one of scheelite ground. If size of pyrrhotite particle is small, magnetic force acting on pyrrhotite particle is small, so it can't float to water surface. Larger size of pyrrhotite particle is, stronger magnetic force is and surface tension of water-air is also smaller. Surface tention of pyrrhotite particle in interface of air-water becomes stronger as size of particle decreases. Large pyrrhotite particles overcome surface resistance and attach to magnet. Therfore, effect of particle size can be and in this study large pyrrhotite particles were used in simulation.

Washing hydraulic force is so small that pyrrhotite particles could still stay, but most of pyrrhotite particles were removed with wash water. Generally, fine minerals is separated in industrical shaking table, the maximum size of particle ground is below 0.5 mm. Thus the size of pyrrhotite is 0.5 mm was considered in simulation.

Then the next major factors are arrangement distance and fixing height of magnets.

The magnetic character of permanent magnets arranged is shown in Figure 11.

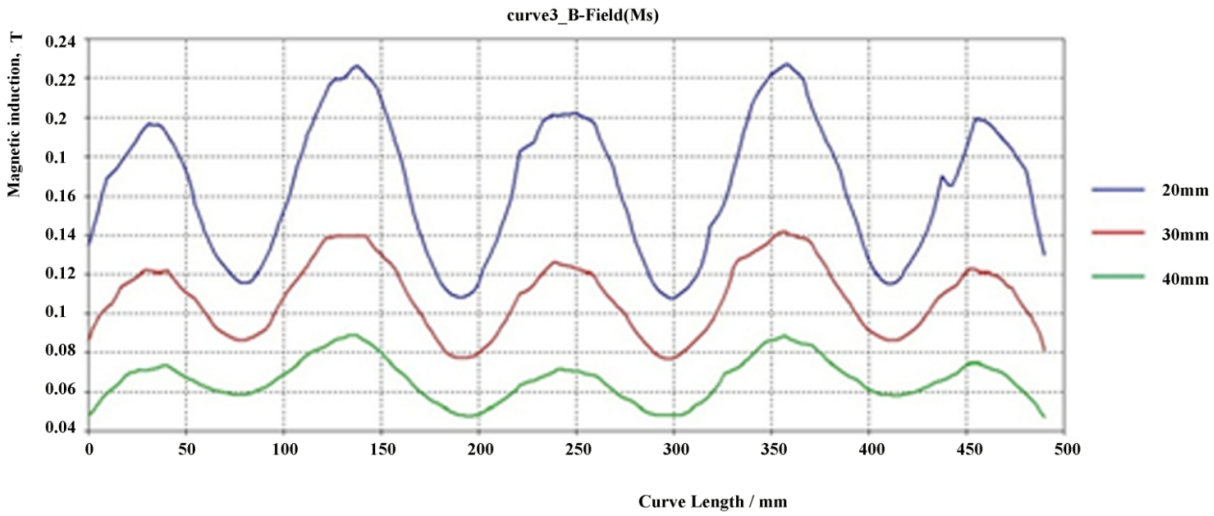

Figure 11. Magnetic induction of permanent magnets arranged.

Magnetic character is related to the arrangement of magnets, and magnetic intensity depends on position in shown Figure 11. Magnetic field is strong in end edges of magnet, but magnet magnetic field is weak in middle of magnet, it depends on arrangement distance of magnets and distance of magnet bar surface.

Pyrrhotite particles around the end edges of magnet can be attached to it, but these in weak field can be settled in water. However, pyrrhotite particles must be not attached to magnet (formulae 2 and 3).

For this condition, arrangement distance of magnets and fixing height of magnets must be determined through simulation. Because washing water flows vertically to riffle direction, fixing angle of magnetic bar must be determined by flow direction of washing water.

To remove floating pyrrhotite particles to tailing over riffles, fixing angle of magnetic bar must be almost vertically to riffle direction. The simulation fixed magnetic bar also was carried in above same condition of quantity of water 4.8 m^3/h, deck slope 2°, strokes per minute 300 mm, length of stroke 12 mm, and feed rate 1.0 t/h. UDF function was used to account for magnatic forces that act on magnetic particles under the existence of magnetic field (formula 1).

Simulation was carried out in 6 cases, which fixing height of magnetic bar is 30 mm, 40 mm, and arrangement distance of magnets is 30 mm, 50 mm, 70 mm.

The simulation result of pyrrhotite removal is shown in Table 2.

Table 2. Results of pyrrotite removal.

Case of simulation	Mass ratio of pyrrotite, %		
	Concentrate	Tailing	Amount attached to magnets
1	1	96	3
2	3	97	0
3	7	93	0
4	1	95	4
5	5	95	0
6	9	91	0

Pyrrhotite particles were successfuly removed in the 2nd case when fixing height of magnetic bar was 50 mm arrangement distance of magnets was 30 mm.

Figure 12 are results of simulation of pyrrhotite removal.

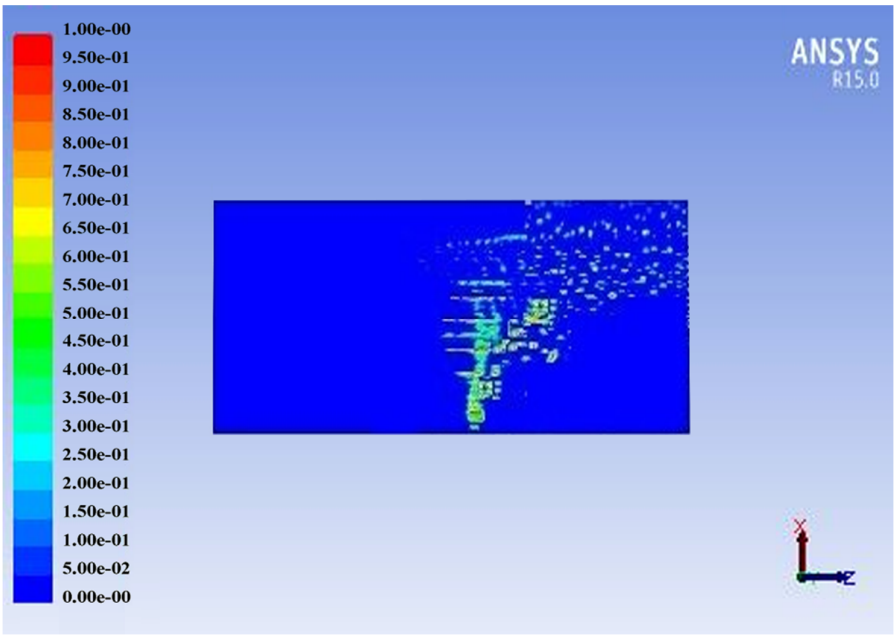

(a)

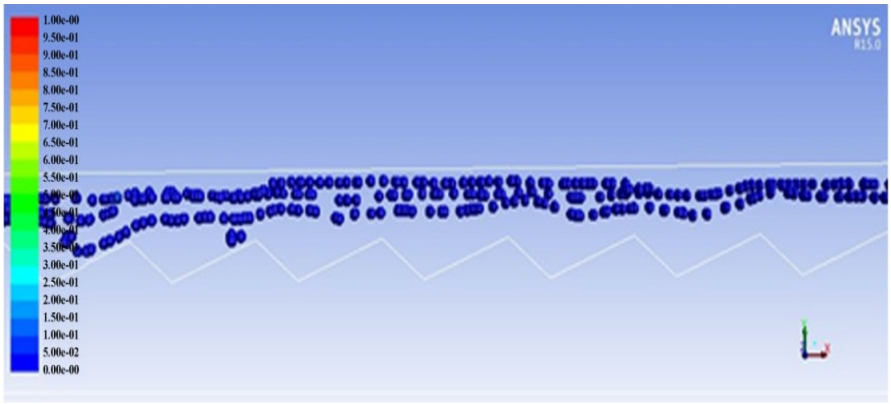

(b)

Figure 12. Removal of pyrrhotite particles by magnets. a) Simulation results of pyrrhotite in time 5s; b) track of pyrrhotite particles.

The motion of pyrrhotite particles is shown Figure 12 a). 97% of pyrrhotite particles were floated by magnetic force without being attached to magnets and washed to tailing flow in this case. Although pyrrhotite also belongs to heavy mineral, pyrrhotite have not reached the concentrate area by magnetic force and flowed along same fixing directionof magnetic bar and went to tailing.

Gravity separation result of scheelite and quartz is similar to conventional table result.

The motion track of pyrrhotite particles floated on desk is shown Figure 12 b). As shown in Figure 12, pyrrhotite particles floated by magnetic force in water and revered to tailing with quartz particles. Because of change of magnetic pole and shaking action of table, none of scheelite into pyrrhotite particles was lost.

4. Discussion

4.1. Separation result

The separation result is characterized by the grade and recovery, but quality and quantity of table separation products are varied according to the position of splilter which divides feed into the concentrate and the tailing. To improve the grade, the splilter should be closer to the concentration launder, but to increase the recovery, it should be closer to the tailing launder.

Therefore, the efficiency of separation (Es) is more appropriate for characterizing the table separation result [36].

$$E_S = R_V - R_g \quad (8)$$

where R_V is the recovery of the valuable mineral, and R_g is the recovery of the gangue into the concentrate.

From data in simulation, the grade of concentrate, recovery and separation efficiency were, respectively, calculated.

Scheelite feed quantity $Q_{fee,sch}$ was calculated from **mass flow rate** of feed **inlet** in **fluxes** of **report** item in simulation. $Q_{fee,sch}$ is Scheelite amount of feed, $Q_{fee,pyr}$ is pyrrhotite amount of feedand, and $Q_{fee,quar}$ is quartz amount of feed. Q_{fee} is amount of feed expressed as sum of $Q_{fee,sch}$, $Q_{fee,sch}$ and $Q_{fee,quar}$.

Scheelite concentrate quantity $Q_{con,sch}$ was calculated from **mass flow rate** of **concentrate outlet** in **fluxes** of **report** item, pyrrhotite quantity $Q_{con,pyr}$ and quartz quantity $Q_{con,quar}$ was also calculatd from the same method. $Q_{con,sch}$ is Scheelite amount of concentrate, $Q_{con,pyr}$ is pyrrhotite amount of concentrate, and $Q_{con,quar}$ is quartz amount of feed. Concentrate amount Q_{con} is sum of $Q_{con,sch}$, $Q_{con,pyr}$ and $Q_{con,quar}$.

Grade WO_3 of concentrate, which is Scheelite mass ratio in concentrate, is follows as:

$$g_{sch} = 80.53 \times \frac{Q_{con,sch}}{Q_{con}} \quad (9)$$

where g_{sch} is the grade WO_3 of scheelite concentrate, and 80.53 is the WO_3 value of scheelite.

Recovery of concentrate follows as:

$$\mathrm{R}_{sch} = \frac{Q_{con,sch}}{Q_{fee,sch}} \times 100\ \% \quad (10)$$

where R_{sch} is scheelite recovery of concentrate.

In the first simulation, grade of concentrate and recovery were, respectively, calculated from data in only conventional gravity concentration. As shown in Figure 3, splitter was set on the end of riffles splitter was set on the end of riffles. Almost all Scheelite and pyrrhotite flowed together to concentrate launder in first simulation. In first simulation, Scheelite feed quantity $Q_{fee,sch}$ was 0.0144 kg/s, Scheelite concentrate quantity $Q_{con,sch}$ was 0.0144 kg/s, pyrrhotite quantity $Q_{con,pyr}$ was 0.0288 kg/s, and concentrate quantity Q_{con} was 0.0432 kg/s.

In simulation, the content of scheelite in feed was 1%, so the theoretical grade in feed was 0.805% WO_3. From formula (9), grade WO3 of scheelite concentrate was 26.84%. Because concentrate is a mixture of scheelite and pyrrhotite, grade of scheelite concentrate was only 26.84% WO_3, and the separation efficiency was 98.0%.

In the second simulation when magnetic bar fixed over table, scheelite particles moved into concentrate launder, pyrrhotite with quartz were removed into tailing launder by water flow in table. From the same calculation of second simulation which magnetic bar fixed on table, Scheelite feed quantity $Q_{fee,sch}$ was 0.0144 kg/s, Scheelite concentrate quantity $Q_{con,sch}$ was 0.0144 kg/s, pyrrhotite quantity $Q_{con,pyr}$ was 0.008 kg/s, and concentrate quantity Q_{con} was 0.0152 kg/s.

From formula (8), Scheelite grade in concentrate in second simulation is 66.29% WO_3, and the separation efficiency was 99.96%.

Two results showed that in the second case the grade was higher than in the first, separation efficiency also was improved more. In simulation, although numerical value is high, comparing two results, the second separation efficiency was higher. This means that combination of gravity and mantetic force on shaking table may improve not only grade but also efficiency.

4.2. Comparision with experiments

To compare the simulation result, table experiments for scheelite ore carried out in the same conditions of simulation.

Firstly, conventional table experiments were conducted. For the experiment, single minerals of scheelite, pyrite and quartz, of which grades are higher than 98%, were ground in laboratory ball mill to -0.5 + 0.04 mm of particles. Mixed ore is composed of 1% of scheelite and 2% of pyrrhotite were used as representative of scheelite from Hocheon area of DPR of Korea with 5×10^{-2} kg of scheelite, 10×10^{-2} kg of pyrrhotite, and 4.85 kg of quartz.

A pilot scale table with a size of 2100 × 1050 mm was used in experimental Wilfley table.

Here, splitter was put on the end of riffle, and other operating parameters such as quantity of water, feed pulp density, deck slope, strokes per minute, length of stroke, and feed rate were same simulation of scheelite concentration.

In first table experiment, which has no magnetic bar, the cumulated concentrate from experimnets weighed 0.1447kg ~ 0.145kg and the the grade was 28.4 % WO_3 in 3 of experiment numbers, and the efficiency of separation was 76.5 % in result.

Next experiment was conducted in the table fixed with magnet bars at a heightof 300 mm above the table desk using the same material. In magnetic bar, Sm-Co magnets, which are Sm_2O_{17} magnets with residual magnetization Br -1.1 T, maximum energy product $(BH)_{max}$ - 300.0 kJ/m^3 arranged space 50 mm in similar condition of the simulation. The position of splitter was same as above experiment and test was repeated 3 times.

The cumulated concentrate from experimnets weighed 0.052 kg ~ 0.0537 kg, and the the grade was 65.5% WO_3 in 3 of experiment numbers. Experimental results, which have magnetic bar showed that the grade was 65.3% WO2, the efficiency of separation was 80.1%.

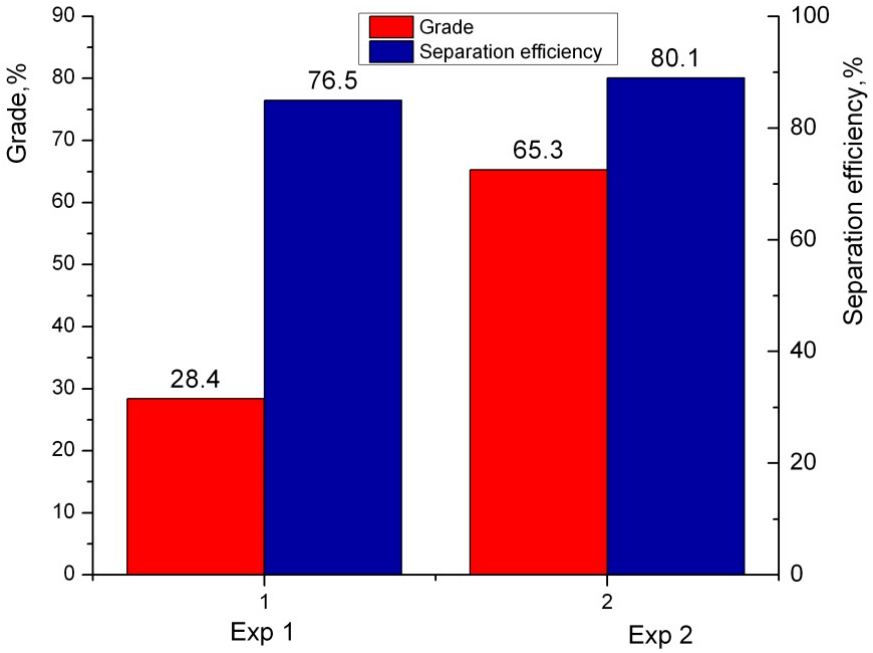

Figure 13. Results of table experiments. Exp. 1 is experiment in conventional table, and Exp. 2 is experiment in table fixed magnetic bar.

Figure 13 showed the results of concentration in two ways.

The grade of concentrate obtained in the first experiment was 28.4% WO_3 and one obtained in the second was 65.3% WO_3, so the latter was higher than first (Figure 13, Exp 1). Separation efficiency in the first experiments was 76.5% and one in the second was 80.1%; as a results, the latter was higher than first (Figure 13, Exp 2).

Results showed that setting of magnetic bar on table with ore increased both the grade of concentrate and separation efficiency.

There were disagreements in grade and separation efficiency obtained from simulations and experiments. These were caused by incomplete description simulations on table experiments, i.e. difference of simulations and table experiments.

Separarion of scheelite, pyrrhotite, and quartz was considered in the simulation. The simulation result showed that scheelite and pyrrhotite could reach the concentrate zone within the simulation time to become concentrate and tailing, whereas concentrate was mixed with gangue minerals in the experiment which was conducted in continuous way.

Although splitter was placed in the same position in both cases, simulation might not have considered this condition. Besides, smaller table size was used in simulation to decrease simulation time. In addition, pure scheelite was considered in simulation, whereas actual sample was used in experiment.

Recovery and separation efficiency could be exaggerated or incorrect in simulation, but they could be comparatively correct in experiment.

However, distinct differences of grade and separation efficiency between in the table fixed with magnet bars and in the conventional one were proved in both cases. Further work will be done to solve the disagreement between simulation and experiment.

5. Conclusions

In this study, a method which heavy valuable mineral was concentrated by gravity while heavy magnetic gangue mineral is removed by forming magnetic field on table desk was studied.

Gravity concentration of scheelite on table and removal of pyrrhotite floated by magnet were simulated using CFD and proved through experiment.

The results of CFD simultion and compared with experiments can be summarized as follows:

a. The simulation result indicated that scheelite was concentrated within 10 s in conventional table and pyrrhotite was separated into tailing within 7s in the magnet bar-fixed table, consequently proving concentration of scheelite by gravity and removal of pyrrhotite by magnetic force.

b. The experiment result showed that grade and separation efficiency were 26.5% and 76.5% in conventional table and 65.3% and 80.1% in the magnet bar-fixed table, respectively. Besides, loss ratio of valuable mineral during table concentration was decreased 2 ~ 3% in the latter case.

c. This method might be useful in replacing sequential table-magnetic separation with single table separation. It could be applicable not only to beneficiation of tin, tangusten, and tantalium ores containing magnetic minerals but also to physical processing of rare metal placer.

Data Availabity

The data used to support the findings of this study is available from the corresponding author upon request.

Conflicts of Interest

The authors declare that they have no conflicts of interest regarding the publication of this paper.

Author Contributions

All authors contributed to the study conception and design. Material preparation, data collection, and analysis were performed by Chol Ung Ryom, Kwang Hyok Pak, Il Chol Sin, Kwang Chol So, and Un Chol Han. The first draft of the manuscript was written by Chol Ung Ryom and Un Chol Han, and all authors commented on previous versions of the manuscript. All authors read and approved the final manuscript.

Acknowledgements

This work was supported by the National Science and Technical Development Foundation of DPR Korea (Grant No. 24-22670527).

References

[1]. Yang , X. (2018). Beneficiation studies of tungsten ores–a review. *Minerals Engineering, 125*, 111–119.

[2]. Schmidt, S. (2012). From Deposit to Concentrate: The Basics of Tungsten Mining Part 2: Operational Practices and Challenges. *Austria: Wolfram Bergbau & Hütten AG*, 22.

[3]. Lassner, E., & Schubert, W. D. (1999). *Tungsten: properties, chemistry, technology of the elements, alloys, and chemical compounds.* Springer Science & Business Media.

[4]. Mohammadnejad, S., Noaparast, M., Hosseini, S., Aghazadeh, S., Mousavinezhad, S. & Hosseini, F. (2018). Physical methods and flotation practice in the beneficiation of a low grade tungsten-bearing scheelite ore. *Russ. J. Non-Ferr. Met.* 59, 6–15.

[5]. Hamid, S. A., Alfonso, P., Oliva, J., Anticoi, H., Guasch, E., Carlos Homann Sampaio, Garcia-Vallès, M. & Escobet, T. (2019). Modeling the Liberation of Comminuted Scheelite using Mineralogical Properties. *Minerals, 9*, 536.

[6]. Anticoi, H., Guasch, E., Hamid, S. A., Oliva, J., Alfonso, P., Garcia-Valles, M. & Peña-Pitarch, E. (2018). Breakage function for HPGR: Mineral and mechanical characterization of tantalum and tungsten ores. *Minerals, 8*(4), 170.

[7]. Miettinen, T., Ralston, J. & Fornasiero, D. (2010). The limits of fine particle flotation. *Minerals Engineering, 23 (5)*, 420–437.

[8]. Zuo, Z. & Gao, Y. (2016). Research advances of the processing technologies for the wolframite-scheelite mixed ore in China. China Tungsten Industry, 31, 253(03), 41-45 (+54).

[9]. Huang *et al*., (2016). Recovery Technology of Poly-metallic Sulfide Ore in China's Tungsten Mines. China Tungsten Industry, 31, 251(01), 58-62+73.

[10]. Becker, M. (2010). The flotation of magnetic and non-magnetic pyrrhotite from selected nickel ore deposits. *Minerals Engineering*, 23, 1045-1052.

[11]. Tarling, D.H. & Hrouda, F. (1993). The Magnetic Anisotropy of Rocks. Chapman & Hall, London, pp. 5-217.

[12]. O'Reilly, W. (1984). Rock and Mineral Magnetism. Blackie & Son, Ltd., Glasgow and London.pp.3-25.

[13]. Wills, B. A. (2016). Mineral Processing Technology Eighth Edition. Mc Gill University, Montreal, Canada, pp. 233-235.

[14]. Carvalho, M. T., Agante, E., & Durão, F. (2007). Recovery of PET from packaging plastics mixtures by wet shaking table. Waste Management, 27(12), 1747-1754.

[15]. Sivamohan, R., & Forssberg, E. (1985). Principles of tabling. International Journal of Mineral Processing, 15(4), 281-295.

[16]. Manser, R. J., Barley, R. W. & Wills, B. A. (1991). The Shaking Table Concentrator - the influence of operating conditions and table parameters on mineral separation-the development of a mathematical model for normal operating conditions. *Minerals Engineering*, 4, 369-381.

[17]. Tucker, P., Lewis, K. A., & Wood, P. (1991). Computer optimisation of a shaking table. *Minerals Engineering*, *4*(3-4), 355-367.

[18]. Razali, R., & Veasey, T. J. (1990). Statistical modelling of a shaking table separator part one. *Minerals Engineering*, *3*(3-4), 287-294.

[19]. Svoboda, J. (2004). *Magnetic techniques for the treatment of materials*. Springer Science & Business Media.

[20]. Martinez, E. (1986). The gravity-magnetic separator: A new development for recovery of weakly magnetic minerals. *In: Advances in Mineral Processing: A half-century of progress in application of theory to practice*. March, New Orleans, La., USA, Chapter 32, pp. 545.

[21]. Lin, I. J., Knish-Bram, M., & Rosenhouse, G. (1997). The benefication of minerals by magnetic jigging, Part 1. Theoretical aspects. *International journal of mineral processing*, *50*(3), 143-159.

[22]. Lin, I. J., Krush-Bram, M., & Rosenhouse, G. (1998). The benefication of minerals by magnetic jigging-Part 1: Theoretical aspects. *International Journal of Mineral Processing*, *54*(1), 29-44.

[23]. Lin, I. J., Krush-Bram, M., & Rosenhouse, G. (1998). The benefication of minerals by magnetic jigging, Part 3. The bed effects and the multifrequency magnetic jig. *International journal of mineral processing*, *55*(1), 61-72.

[24]. Torno, S., Toraño, J., Gent, M., & Menéndez, M. (2011). A study of hydrocyclone classification of coal fines by CFD modeling and laboratory tests. *Mining, Metallurgy & Exploration*, *28*, 102-109.

[25]. Wan, G., Sun, G., Xue, X., & Shi, M. (2008). Solids concentration simulation of different size particles in a cyclone separator. *Powder Technology*, *183*(1), 94-104.

[26]. Viduka, S., Feng, Y., Hapgood, K., & Schwarz, P. (2013). CFD–DEM investigation of particle separations using a sinusoidal jigging profile. *Advanced Powder Technology*, *24*(2), 473-481.

[27]. Xia,Y., Peng, F. F., and Wolfe, E.(2007). CFD simulation of fine coal segregation and stratification in jigs. *J. Miner. Process.* 82, 164–176.

[28]. Rudman, M., Paterson, D. A., & Simic, K. (2010). Efficiency of raking in gravity thickeners. *International Journal of Mineral Processing*, *95*(1-4), 30-39.

[29]. Fatahi,M.R. and Farzanegan, A.(2018). An analysis of multiphase flow and solids separation inside Knelson Concentrator based on four-way coupling of CFD and DEM simulation method. *Minerals Engineering*. 126, 130–144.

[30]. Kannan, A. S., Jareteg, K., Krieger Lassen,N.C., Carstensen, J. M., Edberg Hansen,M.A., Dam, F. and Sasic, S.(2017). Design and performance optimization of gravity tables using a combined CFD-DEM framework. *Powder Technology*. 318, 423-440.

[31]. Gülsoy, Ö. Y., & Gülcan, E. (2019). A new method for gravity separation: Vibrating table gravity concentrator. *Separation and Purification Technology*, *211*, 124-134.

[32]. Pavanello, P., Carrubba, P., & Moraci, N. (2018). The determination of interface friction by means of vibrating table tests. *Geotextiles and Geomembranes*, *46*(6), 830-835.

[33]. Mohanty,S., Das, B. and Mishra, B.K.(2011). A preliminary investigation into magnetic separation process using CFD. *Minerals Engineering*. 24. 1651–1657.

[34]. Derkach, V. G. (1966). Special methods for the beneficiation of minerals. *Nedra, Moscow (in Russian).*

[35]. Walmer, M. S., Chen, C. H., & Walmer, M. H. (2000). A new class of Sm-TM magnets for operating temperatures up to 550/spl deg/C. *IEEE Transactions on Magnetics*, *36*(5), 3376-3381.

[36]. Schulz, N. F. (1970). Separation Efficiency, Society of Mining Engineer. In *AIME* (Vol. 247, pp. 81-87).

شبیه سازی حذف پیروتیت از سنگ معدن شیلیت توسط نیروی مغناطیسی در غلظت جدول

چول اونگ ریوم[1]، کوانگ هیوک پاک[1]، ایل چول سین[1]، کوانگ چول سو[1] و اون چول هان[2*]

1. دانشکده مهندسی معدن، دانشگاه صنعتی کیم چاک، پیونگ یانگ، جمهوری دموکراتیک خلق کره
2. دانشکده علوم و مهندسی، دانشگاه صنعتی کیم چاک، پیونگ یانگ، جمهوری دموکراتیک خلق کره

ارسال 2023/07/21، پذیرش 2023/09/19

* نویسنده مسئول مکاتبات: huch8272@star-co.net.kp

چکیده:

سنگ معدن شیلیت با مواد معدنی سنگین و مغناطیسی را می‌توان به طور کلی با استفاده از پردازش گرانشی-مغناطیسی متمرکز میز تکان دهنده تغلیظ کرد. هنگامی که میدان مغناطیسی با تثبیت میله‌های مغناطیسی که آهن‌رباهای دائمی روی میز قرار گرفته‌اند، در بالای میز تشکیل می‌شود، ذرات شیلیت سنگین را می‌توان توسط گرانش متمرکز کرد، در حالی که ذرات معدنی مغناطیسی سنگین را می‌توان مانند ذرات معدنی سبک توسط مغناطیسی به سمت بالا شناور کرد. زور. در این مقاله غلظت شیلیت و حذف پیروتیت شناور شده توسط نیروی مغناطیسی با استفاده از CFD برای نمونه حاوی 1% شیلیت و 2% پیروتیت شبیه‌سازی و با آزمایش مقایسه شد. در نتیجه، درجه WO3 و راندمان جداسازی کنسانتره در جدول جدید مجهز به میله مغناطیسی به ترتیب 65,3 و 80,1 درصد و در جدول معمولی به ترتیب 28,4 و 76,5 درصد بود. میدان مغناطیسی تشکیل شده توسط تثبیت میله‌های مغناطیسی بالای جدول می‌تواند در ساده سازی فرآیند جداسازی متوالی جدول-مغناطیسی و کاهش از دست دادن اسکیلیت مهم باشد.

کلمات کلیدی: غلظت جدول، Scheelite، Pyrrhotite، نوار مغناطیسی، شبیه سازی CFD.